

Synthesis of Amorphous Monomeric Glass Mixtures for Organic Electronic Applications

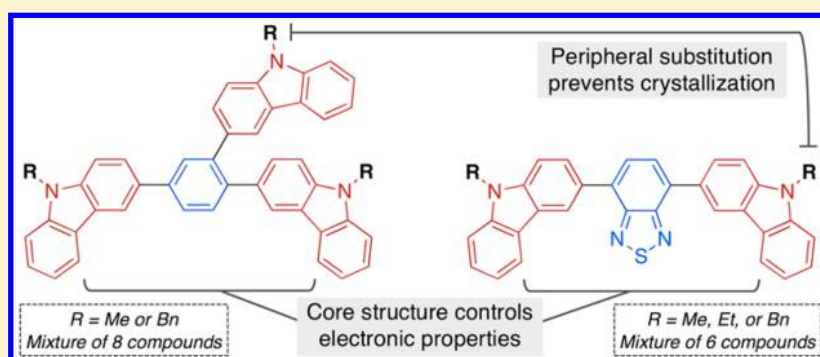
You-Chi Mason Wu,[†] Michel F. Molaire,[‡] David S. Weiss,^{‡,§} Felipe A. Angel,[§] Catherine R. DeBlase,[†] and Brett P. Fors^{*,†}

[†]Department of Chemistry and Chemical Biology, Cornell University, Ithaca, New York 14853, United States

[‡]Molecular Glasses, Incorporated, Rochester, New York 14625, United States

[§]Department of Chemical Engineering, University of Rochester, Rochester, New York 14627, United States

S Supporting Information



ABSTRACT: We report a divergent synthetic strategy and novel design concept that exploit molecular mixtures to create amorphous organic charge-transporting glasses. Using Suzuki–Miyaura cross-coupling reactions, we synthesized well-defined molecular mixtures in a single step. These solution-processable materials are noncrystalline and show good thermal and morphological stabilities. Moreover, they have robust hole and electron mobilities, which make them excellent candidate materials for organic light-emitting diodes. Our general strategy enables the facile synthesis of noncrystalline materials with well-controlled electronic properties.

Low molecular weight organic compounds that form stable amorphous phases are of interest as materials for organic light-emitting diodes (OLEDs),^{1,2} organic photovoltaics,³ electrophotography,⁴ photorefractive applications,⁵ and photoresists.⁶ Therefore, the development of charge-transporting molecular glasses that show high morphological and thermal stability has been an active area of research.^{4,7} Many compounds form amorphous films through vitrification processes; however, they often have low morphological stability and can crystallize over time, impairing device performance.^{2,8} To prevent crystallization, researchers have designed molecules with nonplanar geometries or bulky substituents or have switched to polymeric systems, all of which sacrifice the processability or electronic properties of these materials.⁴ As a result, the development of a general strategy to synthesize truly noncrystallizable molecular glasses that have tunable electronic properties and retain excellent processability is both a major opportunity and a grand challenge in this field.

To address this challenge, we took advantage of organic monomeric glasses introduced by researchers at Eastman Kodak Company.⁹ Molaire and Johnson have demonstrated that materials with infinitely low crystallization rates can be predictably synthesized by designing a mixture of compounds that contain core structures that vary slightly in their peripheral

substitution patterns. These mixtures are readily soluble in organic solvents and form homogeneous amorphous films that are stable well above room temperature. We hypothesized that this design approach could be a general and modular strategy for making noncrystallizable charge-transporting glasses. The core structure of these mixtures would allow the tuning of the electronic properties of the material, and the peripheral substitution would control crystallinity, solubility, and chemical compatibility (Figure 1).

To render this approach viable, we pursued a divergent and general synthetic strategy for making charge-transporting molecular glasses. Because the synthesis and blending of individual components would be impractical, we sought a single-pot reaction to construct the core molecular structure while forming statistical mixtures of various substitution patterns (Figure 2). This approach would allow the predictable formation of well-defined compositions in a single step. We reasoned that the selected reaction must meet several criteria. First, substrates with various substituents must react at the same rate to ensure stochastic distributions of the different

Received: October 24, 2015

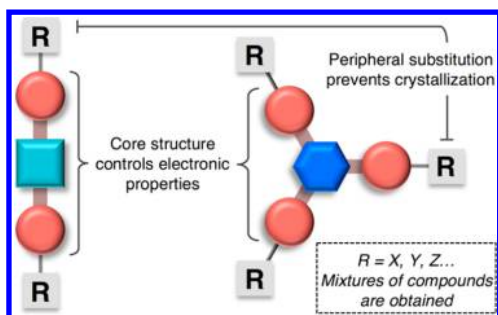


Figure 1. General design strategy for amorphous charge-transporting glasses.

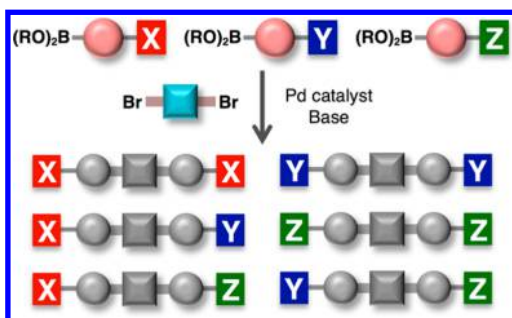


Figure 2. Synthetic strategy using Suzuki–Miyaura coupling reactions to give monomeric glasses with stochastic substitution combinations.

components. Second, the products must be purified through methods such as extraction and precipitation; chromatography of a mixture has the potential to be difficult, and the noncrystallinity of the products excludes the use of recrystallization. Third, near quantitative yields and minimal side product formation is necessary. We envisaged that the Suzuki–Miyaura cross-coupling reaction would be an ideal candidate for the synthesis of these charge-transporting materials because it fits the above criteria and enables the efficient formation of the extended aromatic systems needed for these materials.^{10,11}

To test our strategy, we synthesized two separate monomeric glass mixtures with different electronic characteristics—a hole-transport material and an ambipolar charge-transporting material. For the former, we coupled 1,2,4-trichlorobenzene with a 1:1 mixture of the 9-methyl- and 9-benzylcarbazole-3-boronate pinacol esters by using a Pd catalyst based on the ligand XPhos.¹² We hypothesized that the small structural variation in the carbazoles would not influence the rate of transmetalation for these reactions, which would afford a stochastic distribution of eight compounds containing various *N*-methyl and *N*-benzyl substitutions. After stirring at 40 °C for 16 h, the reaction was washed with water, filtered through a plug of silica, and precipitated in hexanes to give pure molecular glass mixture **1** in 90% yield (Figure 3a). ¹H NMR data confirmed the correct ratio of methyl and benzyl substituents. Additionally, liquid chromatography–mass spectrometry (LC-MS) data provided the masses of all eight compounds in the appropriate molar proportions (Figure 3b).

Using an analogous reaction to that above, we coupled 4,7-dibromobenzothiadiazole with a 1:1:1 mixture of 9-methyl-, 9-ethyl-, and 9-benzylcarbazole-3-boronate pinacol esters to give ambipolar molecular glass **2** in 75% yield after precipitation (Figure 4a).¹³ The results of ¹H NMR and LC-MS confirmed the presence of the six expected compounds in the appropriate

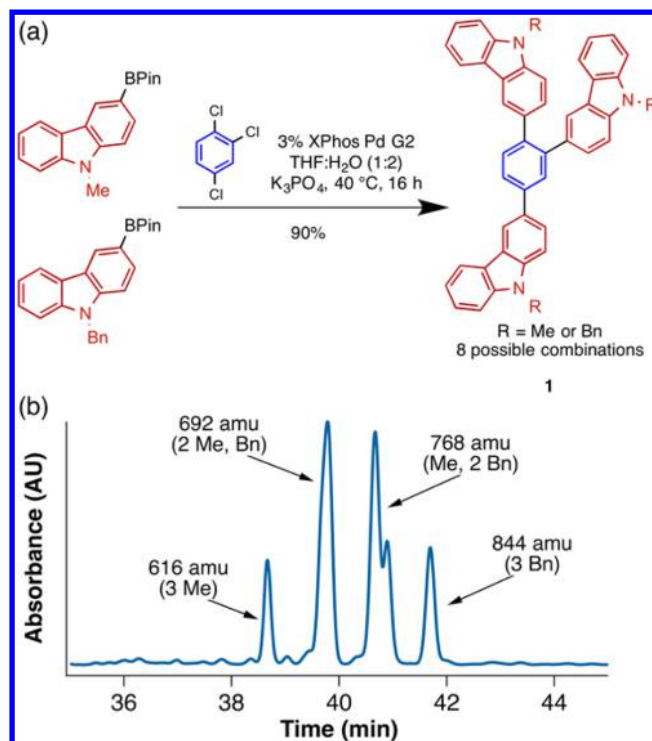


Figure 3. (a) Suzuki–Miyaura cross-coupling to give hole-transport material **1**, and (b) LC-MS data identifying the eight components of the molecular glass.

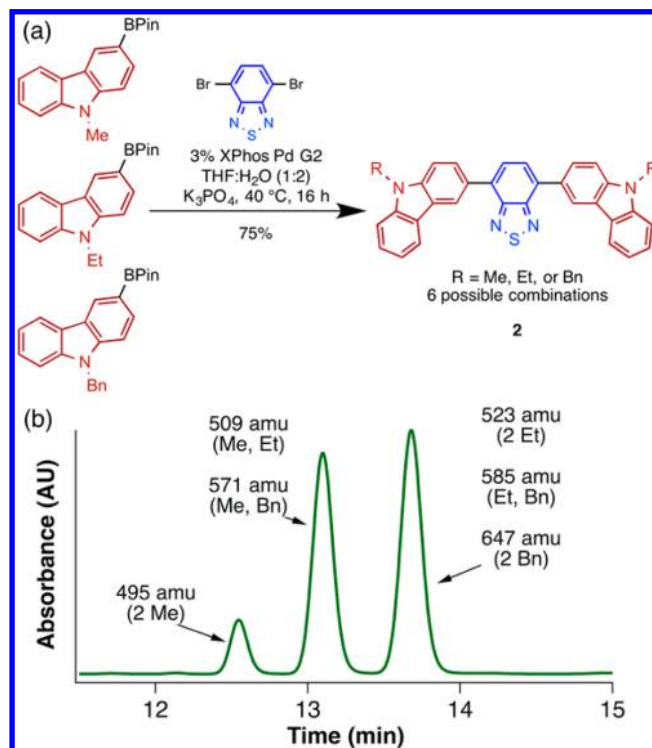


Figure 4. (a) Suzuki–Miyaura cross-coupling to give ambipolar transport material **2** and (b) LC-MS data identifying the six components of the molecular glass.

ratios (Figure 4b). Notably, three *N*-substituted carbazoles were used to synthesize this material to help disrupt the symmetry of the disubstituted molecular core to prevent crystallization. These results corroborate the viability of this divergent strategy

and illustrate that the Suzuki–Miyaura reaction can provide well-defined molecular glass mixtures in a single step with minimal purification.

Differential scanning calorimetry (DSC) was used to characterize the morphology of the two monomeric molecular glasses.^{14,15} Performing multiple heating and cooling cycles at 10 °C/min revealed glass transition temperatures (T_g 's) of 140 and 106 °C for **1** and **2**, respectively (Figure 5). These values

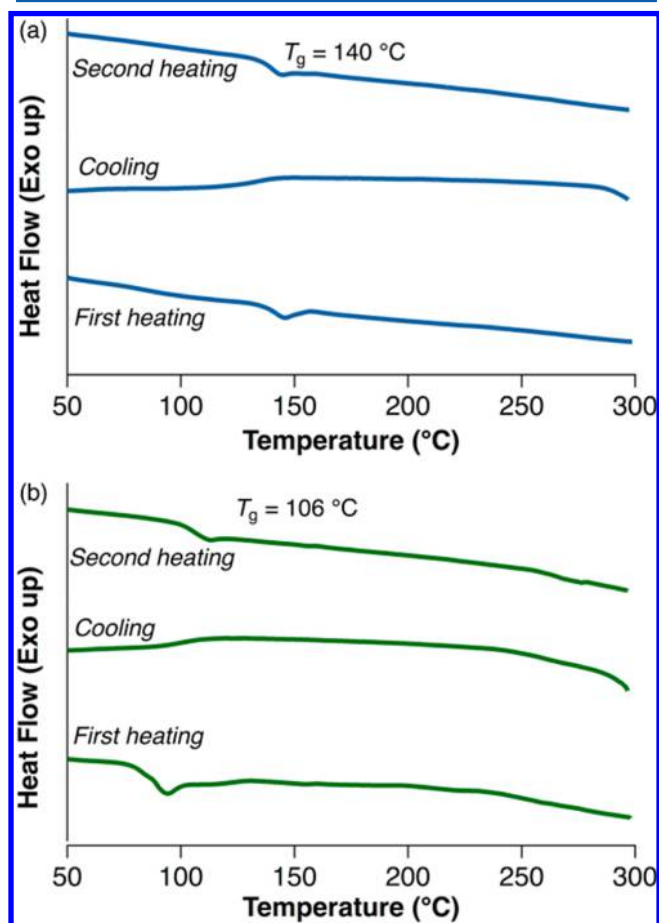


Figure 5. Differential scanning calorimetry (DSC) heat/cool/heating curves of (a) **1** and (b) **2** performed at 10 °C/min. No crystallization was observed for either material.

are significantly higher than those of other charge transport materials that can be trapped in a glassy state, such as the hole-transport material *N,N'*-bis(3-methylphenyl)-*N,N'*-diphenylbenzidine ($T_g = 65$ °C).¹⁶ Significantly, upon heating above the T_g , neither material showed crystallization, which

demonstrated that these mixtures are noncrystalline.¹⁷ To support this conclusion, we performed the same DSC experiments at slower cooling rates of 1 °C/min, which provided more favorable crystallization conditions.¹⁸ Again, no crystallization was observed for either material, further establishing that these mixtures form materials with stable amorphous phases. In addition to the excellent morphological stabilities of these materials, thermogravimetric analysis of the samples indicated high thermal stability with decomposition onsets at 350 °C for **1** and 330 °C for **2**.

To highlight that the molecular mixtures are crucial to the noncrystallinity of these materials, we synthesized the completely *N*-methyl-substituted congeners of **1** and **2** (Figure 6). The results of DSC experiments showed that both compounds exhibit crystallinity. Additionally, even though they could be trapped in the amorphous state through vitrification, they nonetheless readily recrystallized and then melted upon reheating past their respective T_g 's. These results indicate that the molecular mixtures are critical to the stable amorphous nature of these materials.

The processability of these materials is key for their viability in various applications.^{9,19} Both **1** and **2** are readily soluble in organic solvents (e.g., dichloromethane, tetrahydrofuran, chloroform, and acetonitrile), which makes them amenable to solution processing. Additionally, both **1** and **2** can be thermally deposited as thin films, which is a major advantage over polymeric systems and is important for OLED applications.^{2,20}

Thermal deposition also allows for the measurement of the hole and electron mobilities of the glasses. Electroactive materials require robust charge carrier mobility for high-performance devices.⁷ Using the time-of-flight method, we measured the hole mobilities of **1** and **2** as 1.3×10^{-4} and 1.8×10^{-4} $\text{cm}^2 \text{V}^{-1} \text{s}^{-1}$, respectively. The electron mobility of **2** was 1.2×10^{-4} $\text{cm}^2 \text{V}^{-1} \text{s}^{-1}$. These values are comparable to common hole- and electron-transport materials, clearly demonstrating that the electronic properties of the material can be tuned through the choice of the core structure.^{1,2} Additionally, the electronic and optical properties of **1** and **2** were investigated. The absorption and emission spectra were measured in solution and as thin films, and the highest occupied/lowest unoccupied molecular orbital levels and band gaps of **1** and **2** were characterized with cyclic voltammetry and UV–visible spectroscopy (see Supporting Information).^{21,22} Importantly, the absorption and emission spectra of **1** and **2** are nearly identical to their respective discrete congeners **3** and **4**, suggesting that the electronic properties of the materials are largely controlled by the choice of core structure and are unchanged by the use of a mixture of substituents, whereas the morphological properties are significantly improved.

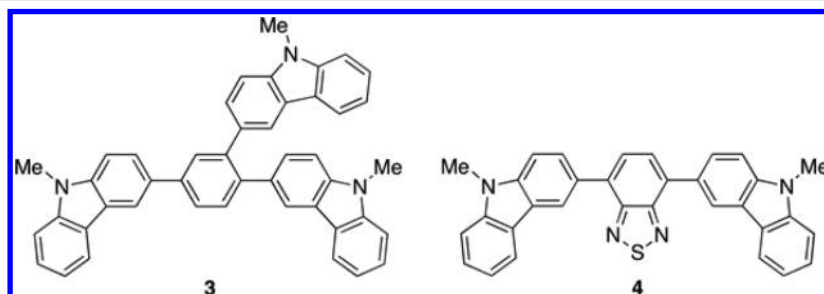


Figure 6. Completely *N*-methyl-substituted congeners of **1** and **2**. DSC analysis showed that both compounds exhibit crystallinity.

To function in OLED devices as a host material for the emitting layer, ambipolar material **2** must be compatible with an emitter while maintaining its amorphous character. To test this capability, we doped **2** with 10, 20, and 40% (w/w) coumarin-6, a common green emitter,²³ and analyzed the samples with DSC. After initial melting of the crystalline dopant during the first heating, no crystallization was detected in any sample during four subsequent heat/cool cycles (Figure 7). This outcome clearly shows that **2** is compatible with coumarin-6 and remains a stable amorphous material even at emitter content beyond commonly used levels.

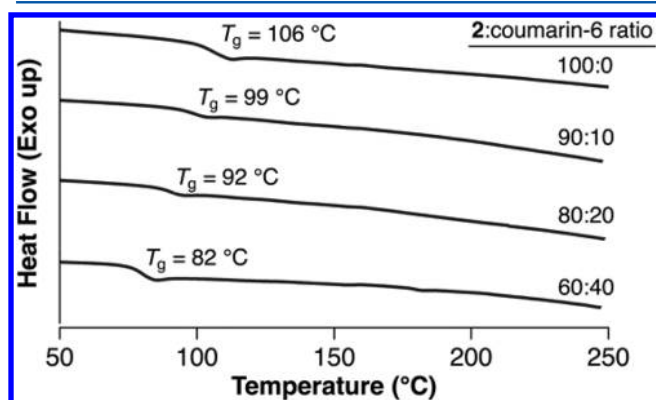


Figure 7. DSC studies of molecular glass **2** doped with coumarin-6. Second heating curves shown for various dopant contents.

As a proof-of-concept that our amorphous mixtures can be successfully utilized in a device, **2** was used as an electron-transport layer in the fabrication of an OLED [ITO/MoOx/NPB/**2**/LiF/Al, where NPB (*N,N'*-di(1-naphthyl)-*N,N'*-diphenyl-(1,1'-biphenyl)-4,4'-diamine) was used as a hole-transport material]. Electroluminescence (EL), current density, luminance, and external quantum efficiency (EQE) data are presented in Figure 8, demonstrating that current transits the device. The OLED produces orange-yellow light with maximum EL at 608 nm. The EQE increases with increasing current density and levels off at 0.34% with a slight decrease at higher current densities. These results demonstrate that amorphous mixtures are suitable materials for OLED

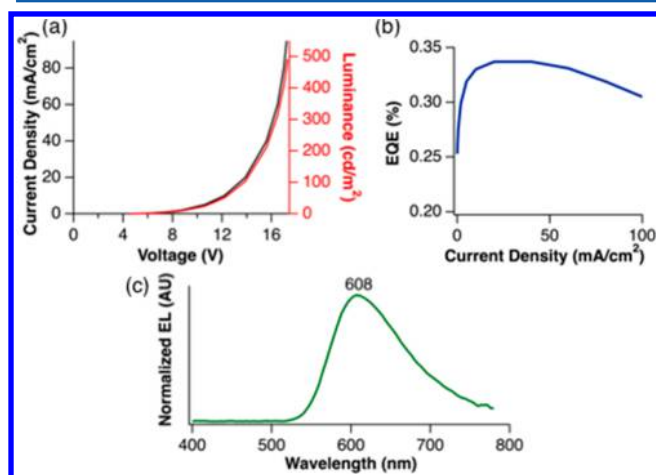


Figure 8. ITO/MoOx/NPB/**2**/LiF/Al device. (a) Current density and luminance characteristics. (b) EQE data with a maximum of 0.34%. (c) EL spectrum of the device with $\lambda_{\text{max}} = 608$ nm.

fabrication. We anticipate that our divergent synthetic strategy can be applied in the further investigation of novel charge-transport materials and can improve device performance through the selection of core and peripheral structures.

In summary, we developed a general and modular strategy for synthesizing amorphous charge-transporting molecular glasses. This divergent strategy uses Suzuki–Miyaura cross-coupling reactions to make well-defined molecular mixtures in a single step. Crucially, the molecular mixtures give rise to materials with high morphological stability, maintaining their amorphous nature even at high temperatures. The materials are solution-processable and amenable to thermal deposition and have robust hole and electron mobilities. Additionally, ambipolar material **2** offers compatibility with crystalline dopants without loss of noncrystallinity. The versatile reaction scheme readily affords diverse products, including the hole-transport and ambipolar charge-transport materials in this study, and we believe this general strategy will be useful for the development of additional amorphous materials with promising potential for electronic applications.

EXPERIMENTAL SECTION

General Methods and Materials. All chemicals were used as received from commercial sources, except for tetrahydrofuran, which was purified by vigorous purging with argon for 2 h, followed by passage through two packed columns of neutral alumina. All reactions were carried out under nitrogen atmosphere in sealed Schlenk tubes. Filtrations were performed using silica gel with a mean pore size of 60 Å and particle size of 63–200 μm . NMR spectra were taken using a 300 MHz instrument in CDCl_3 solvent. All ^1H NMR spectra are reported in δ units (ppm) relative to the residual chloroform signal (7.26 ppm) in the deuterated solvent. All ^{13}C NMR spectra were obtained with ^1H decoupling and are reported in ppm units relative to the chloroform signal (77.16 ppm). All IR spectra were taken neat using an FT-IR spectrometer with an attenuated total reflection attachment. Liquid chromatography–mass spectrometry (LC-MS) data were obtained using acetonitrile/water as the eluent and atmospheric pressure chemical ionization (ACPI) with a multimode quadrupole analyzer. High resolution mass spectrometry (HRMS) was performed using an electrospray ionization source with an orbitrap mass analyzer; reported values are within 3 ppm of the calculated values. All differential scanning calorimeter (DSC) data were taken using standard aluminum pans with heating and cooling rates of 10 $^\circ\text{C}$ per minute from -10 to 300 $^\circ\text{C}$, unless otherwise stated. Thermogravimetric analyzer (TGA) experiments were carried out using a 10 $^\circ\text{C}$ per minute ramp from 25 to 600 $^\circ\text{C}$ in a platinum pan. Thermal deposition was performed with a thermal bell jar evaporator while heating in an alumina crucible. Hole and electron mobility data was obtained using the time-of-flight method. The samples were vacuum-deposited on indium tin oxide glass with a film thickness of approximately 2 μm . Charge generation was accomplished with a pulsed nitrogen laser (337 nm) and mobilities were measured at 2.5×10^5 V/cm. Absorption and fluorescence data were collected using a UV–vis–NIR spectrophotometer and a spectrofluorometer, respectively. Solution spectra were taken in a quartz cuvette using dichloromethane as the solvent, and thin film spectra were obtained of samples that were vacuum-deposited on quartz glass. All cyclic voltammograms (CVs) were executed using a platinum counter electrode and gold working electrode with a 50 mV/s scan rate. The samples were prepared as 1 mM solutions in 0.1 M tetrabutylammonium hexafluorophosphate in acetonitrile. Reported voltages are referenced against a Ag/AgClO₄ electrode. The OLED device was fabricated with the following structure: ITO/MoOx(5 nm)/NPB(75 nm)/**2**(75 nm)/LiF(1 nm)/Al(100 nm).

Molecular Mixture 1. 9-Benzylcarbazole-3-boronic acid pinacol ester (316 mg, 0.825 mmol), 9-methylcarbazole-3-boronic acid pinacol ester (253 mg, 0.825 mmol), and XPhos Pd G2 (35 mg, 3 mol %)

were added to a Schlenk tube, which was fitted with a rubber septum and evacuated and backfilled with nitrogen (the evacuation and backfilling process was repeated a total of three times). 1,2,4-Trichlorobenzene (63 μ L, 0.5 mmol), THF (3 mL), and 0.5 M K_3PO_4 (6 mL), which was degassed by sparging with nitrogen for 20 min, were added to the reaction vessel via syringe. Under positive pressure of nitrogen, the rubber septum was removed, and the flask was sealed with a Teflon screw cap. The solution was heated to 40 °C for 16 h while stirring. Subsequently, the reaction was cooled to room temperature, and the reaction mixture was extracted with dichloromethane (10 mL \times 3). The combined organic phases were filtered through a plug of silica gel and then concentrated in vacuo. The resulting solid was dissolved in a small amount of dichloromethane and precipitated out of 150 mL of heptanes. The precipitate was filtered and dried under vacuum to give the title compound as a white solid (343 mg, 90%). 1H NMR (300 MHz, $CDCl_3$): δ 8.49 (d, J = 6.2 Hz, 2H), 8.26–7.76 (m, 16H), 7.72 (dd, J = 7.9, 1.7 Hz, 2H), 7.56–7.02 (m, 43H), 5.57 (s, 2H), 5.43 (s, 4H), 3.91 (s, 3H), 3.77 (s, 6H) ppm. ^{13}C NMR (75 MHz, $CDCl_3$): δ 141.8, 141.7, 141.5, 141.2, 141.1, 140.9, 140.6, 140.2, 139.8, 139.7, 139.5, 137.1, 131.7, 130.1, 128.8, 128.7, 128.6, 128.4, 127.5, 127.4, 126.5, 126.4, 126.0, 125.9, 125.7, 125.5, 125.3, 123.6, 123.2, 122.9, 122.7, 121.5, 120.5, 119.4, 119.2, 119.0, 118.9, 118.8, 109.2, 109.1, 108.9, 108.8, 108.4, 108.2, 107.8, 46.7, 46.6, 29.2, 29.1. HRMS (ESI⁺, CH_3OH) m/z : [M]⁺ calcd for $C_{45}H_{33}N_3$, $C_{51}H_{37}N_3$, $C_{57}H_{41}N_3$, and $C_{63}H_{45}N_3$ are 615.2674, 691.2987, 767.3300, and 843.3613, respectively; found: 615.2653, 691.2963, 767.3275, and 843.3590. IR (ATR, cm^{-1}): 3046, 2929, 1627, 1599, 1480, 1459, 1330, 1299, 1263, 1246, 1210, 1153, 1123, 1028, 1002, 881, 801, 744, 726, 695, 668, 631.

Molecular Mixture 2. 4,7-Dibromobenzothiadiazole (294 mg, 1.0 mmol), 9-methylcarbazole-3-boronic acid pinacol ester (215 mg, 0.7 mmol), 9-ethylcarbazole-3-boronic acid pinacol ester (225 mg, 0.7 mmol), 9-benzylcarbazole-3-boronic acid pinacol ester (268 mg, 0.7 mmol), and XPhos Pd G2 (47 mg, 3 mol %) were added to a Schlenk tube, which was fitted with a rubber septum and evacuated and backfilled with nitrogen (the evacuation and backfilling process was repeated a total of three times). Dry THF (3 mL) and 0.5 M K_3PO_4 (6 mL), which was degassed by sparging with nitrogen for 20 min, were added to the reaction vessel via syringe. Under positive pressure of nitrogen, the rubber septum was removed, and the flask was sealed with a Teflon screw cap. The solution was heated to 40 °C for 16 h while stirring. Subsequently, the reaction was cooled to room temperature, and the reaction mixture was extracted with dichloromethane (10 mL \times 3). The combined organic phases were filtered through a plug of silica and then concentrated in vacuo. The resulting solid was dissolved in a small amount of dichloromethane and precipitated out of 150 mL of heptanes. The precipitate was filtered and dried under vacuum to give the title compound as an orange solid (413 mg, 75%). 1H NMR (300 MHz, $CDCl_3$): δ 8.76 (dt, J = 9.8, 1.8 Hz, 3H), 8.31–8.05 (m, 6H), 7.88 (m, 3H), 7.62–7.15 (m, 17H), 5.54 (s, 2H), 4.41 (q, J = 7.2 Hz, 2H), 3.87 (s, 3H), 1.49 (t, J = 7.2 Hz, 3H). ^{13}C NMR (75 MHz, $CDCl_3$): δ 154.6, 141.5, 141.1, 140.9, 140.6, 140.4, 139.9, 137.1, 133.2, 129.0, 128.8, 128.6, 128.5, 128.0, 127.9, 127.6, 127.4, 127.2, 126.5, 126.1, 125.9, 123.4, 123.3, 123.1, 123.0, 121.3, 121.2, 120.7, 120.6, 119.5, 119.2, 119.1, 109.1, 109.0, 108.7, 108.5, 46.7, 37.7, 29.2, 13.9. HRMS (ESI⁺, CH_3OH) m/z : [M]⁺ calcd for $C_{32}H_{22}N_4S$, $C_{33}H_{24}N_4S$, $C_{34}H_{26}N_4S$, $C_{38}H_{26}N_4S$, $C_{39}H_{28}N_4S$, and $C_{44}H_{30}N_4S$ are 494.1565, 508.1722, 522.1878, 570.1878, 584.2035, and 646.2191, respectively; found: 494.1547, 508.1704, 522.1873, 570.1858, 584.2014, and 646.2168. IR (ATR, cm^{-1}): 3046, 2929, 1627, 1598, 1460, 1380, 1345, 1328, 1247, 1231, 1211, 1154, 1123, 1057, 1022, 892, 848, 800, 745, 727, 695, 631.

Compound 3. In an analogous procedure to 1, 9-methylcarbazole-3-boronic acid pinacol ester (492 mg, 1.6 mmol), XPhos Pd G2 (35 mg, 3 mol %), 1,2,4-trichlorobenzene (63 μ L, 0.5 mmol), THF (3 mL), and 0.5 M K_3PO_4 (6 mL) were heated to 40 °C for 16 h. The concentrated extract was filtered through a plug of silica and precipitated out of 150 mL of hexanes. The precipitate was filtered and dried under vacuum to give the title compound as a light gray solid (247 mg, 80%). 1H NMR (300 MHz, $CDCl_3$): δ 8.49 (s, 1H),

8.25–8.14 (m, 3H), 8.08–7.97 (m, 3H), 7.95–7.81 (m, 2H), 7.73 (d, J = 7.9 Hz, 1H), 7.57–7.08 (m, 14H), 3.90 (s, 3H), 3.77 (s, 3H), 3.76 (s, 3H). ^{13}C NMR (75 MHz, $CDCl_3$): δ 141.8, 141.5, 141.2, 140.7, 140.6, 139.8, 139.7, 139.6, 133.1, 132.6, 132.0, 131.7, 130.1, 128.4, 125.9, 125.8, 125.5, 125.3, 122.9, 122.7, 121.5, 121.4, 120.5, 120.4, 120.3, 119.0, 118.8, 108.7, 108.6, 108.4, 107.8, 107.7, 29.2, 29.1. HRMS (ESI⁺, CH_3OH) m/z : [M]⁺ calcd for $C_{45}H_{33}N_3$ 615.2674; found: 615.2658. IR (ATR, cm^{-1}): 3048, 2928, 1628, 1600, 1481, 1458, 1424, 1358, 1331, 1245, 1154, 1123, 1065, 1019, 927, 886, 854, 802, 729, 641, 545.

Compound 4. In an analogous procedure to 2, 4,7-dibromobenzothiadiazole (294 mg, 1.0 mmol), 9-methylcarbazole-3-boronic acid pinacol ester (645 mg, 2.1 mmol), XPhos Pd G2 (47 mg, 3 mol %), THF (3 mL), and 0.5 M K_3PO_4 (6 mL) were heated to 40 °C for 16 h. The concentrated extract was filtered through a plug of silica and precipitated out of 150 mL of hexanes. The precipitate was filtered and dried under vacuum to give the title compound as an orange solid (419 mg, 85%). 1H NMR (300 MHz, $CDCl_3$): δ 8.72 (s, 2H), 8.24–8.14 (m, 4H), 7.93 (s, 2H), 7.62–7.43 (m, 6H), 7.32–7.26 (m, 2H), 3.93 (s, 6H). ^{13}C NMR (75 MHz, $CDCl_3$): δ 154.7, 141.5, 140.9, 133.4, 128.6, 127.9, 127.2, 125.9, 123.2, 123.0, 121.2, 120.6, 119.1, 108.6, 108.5, 29.3. HRMS (ESI⁺, CH_3OH) m/z : [M]⁺ calcd for $C_{32}H_{22}N_4S$ 494.1565; found: 494.1550. IR (ATR, cm^{-1}): 3051, 2920, 1629, 1598, 1467, 1426, 1322, 1274, 1245, 1151, 1123, 1058, 1023, 868, 841, 813, 731, 643, 626, 552.

■ ASSOCIATED CONTENT

📄 Supporting Information

The Supporting Information is available free of charge on the ACS Publications website at DOI: 10.1021/acs.joc.5b02459.

1H NMR and ^{13}C NMR spectra of 1–4 and physical and electronic data, including DSC studies, TGA studies, vapor deposition studies, UV–vis and fluorescence spectroscopy, and cyclic voltammetry (PDF)

■ AUTHOR INFORMATION

✉ Corresponding Author

*E-mail: bpf46@cornell.edu.

Notes

The authors declare no competing financial interest.

■ ACKNOWLEDGMENTS

This work was funded by the Cornell Center for Materials Research (CCMR) JumpStart Program supported by Empire State Development's Division of Science, Technology and Innovation and Molecular Glasses, Incorporated, and made use of the CCMR shared facilities, which are supported through the National Science Foundation MRSEC program (DMR-1120296). Y.M.W., C.R.D., and B.P.F. acknowledge Cornell University for support.

■ REFERENCES

- (1) Tao, Y.; Yang, C.; Qin, J. *Chem. Soc. Rev.* **2011**, *40* (5), 2943–2970.
- (2) Shirota, Y.; Kageyama, H. *Chem. Rev.* **2007**, *107* (4), 953–1010.
- (3) Bach, U.; Lupo, D.; Comte, P.; Moser, J. E.; Weissörtel, F.; Salbeck, J.; Spreitzer, H.; Grätzel, M. *Nature* **1998**, *395* (6702), 583–585.
- (4) Stroehriegel, P.; Grazulevicius, J. V. *Adv. Mater.* **2002**, *14* (20), 1439–1452.
- (5) Zilker, S. J. *ChemPhysChem* **2000**, *1* (2), 72–87.
- (6) Yang, D.; Chang, S. W.; Ober, C. K. *J. Mater. Chem.* **2006**, *16* (18), 1693.
- (7) Shirota, Y. *J. Mater. Chem.* **2005**, *15* (1), 75.

- (8) Duan, L.; Hou, L.; Lee, T.-W.; Qiao, J.; Zhang, D.; Dong, G.; Wang, L.; Qiu, Y. *J. Mater. Chem.* **2010**, *20* (31), 6392.
- (9) Molaire, M. F.; Johnson, R. W. *J. Polym. Sci., Part A: Polym. Chem.* **1989**, *27*, 2569–2592.
- (10) Martin, R.; Buchwald, S. L. *Acc. Chem. Res.* **2008**, *41* (11), 1461–1473.
- (11) Bonvallet, P. A.; Breitzkreuz, C. J.; Kim, Y. S.; Todd, E. M.; Traynor, K.; Fry, C. G.; Ediger, M. D.; McMahon, R. J. *J. Org. Chem.* **2007**, *72* (26), 10051–10057.
- (12) Kinzel, T.; Zhang, Y.; Buchwald, S. L. *J. Am. Chem. Soc.* **2010**, *132* (40), 14073–14075.
- (13) Ding, G.; Zhou, H.; Xu, J.; Lu, X. *Chem. Commun.* **2014**, *50* (6), 655–657.
- (14) Shirota, Y. *J. Mater. Chem.* **2000**, *10* (1), 1–25.
- (15) Dawson, K.; Kopff, L. A.; Zhu, L.; McMahon, R. J.; Yu, L.; Richert, R.; Ediger, M. D. *J. Chem. Phys.* **2012**, *136* (9), 094505.
- (16) O'Brien, D. F.; Burrows, P. E.; Forrest, S. R.; Koene, B. E.; Loy, D. E.; Thompson, M. E. *Adv. Mater.* **1998**, *10* (14), 1108–1112.
- (17) Dawson, K.; Zhu, L.; Kopff, L. a.; McMahon, R. J.; Yu, L.; Ediger, M. D. *J. Phys. Chem. Lett.* **2011**, *2* (21), 2683–2687.
- (18) Doi, H.; Kinoshita, M.; Okumoto, K.; Shirota, Y. *Chem. Mater.* **2003**, *15* (5), 1080–1089.
- (19) Keawin, T.; Sooksai, C.; Prachumrak, N.; Kaewpuang, T.; Muenmart, D.; Namuangruk, S.; Jungsuttiwong, S.; Sudyoadsuk, T.; Promarak, V. *RSC Adv.* **2015**, *5* (21), 16422–16432.
- (20) LC-MS analysis of the thin films indicated a small change in ratios of individual components with lower molecular weight components undergoing slightly preferential deposition, but such a change was not expected to impact the morphological or chemical properties.
- (21) Sarsah, S. R. S.; Lutz, M. R.; Zeller, M.; Crumrine, D. S.; Becker, D. P. *J. Org. Chem.* **2013**, *78* (5), 2051–2058.
- (22) Thirion, D.; Rault-Berthelot, J.; Vignau, L.; Poriel, C. *Org. Lett.* **2011**, *13* (16), 4418–4421.
- (23) Tang, C. W.; Vanslyke, S. a.; Chen, C. H. *J. Appl. Phys.* **1989**, *65* (9), 3610–3616.